Strain Developed Around Dental Implants Loaded With Two CAD-CAM Reinforced Polymeric Superstructure Materials: An In-Vitro Comparative Study

Zainab M. Kandeel [1]* *BDs* Ahmed M. Abdelhamid [2] *BDS,* Msc, *PhD,*
Akram F. Neena [3] *BDS, Msc, PhD*

ABSTRACT

INTRODUCTION: Evaluation of strain developed around implants is playing an important role in the success of osseointegration of implants. Among the factors that affect the strain development, we can include the superstructure material.
OBJECTIVE: The present study used strain gauge to perform an in-vitro evaluation of strain development around dental implants after using two different CAD-CAM reinforced polymers as superstructure materials.
MTERIALS AND METHODS: Sixteen polyurethane test blocks were divided into two groups according to the superstructure material, biocompatible high-performance polymer (BioHPP) and reinforced nano-hybrid polymer with multi-layered glass fiber (TRINIA). Superstructures were fabricated with the same design using computerized aiding design then milling from CAD-CAM blocks. Strain gauges measured microstrain values. A universal testing machine was used to apply static load from 0 to 100 N in axial and 45-degree oblique directions on the superstructure. Then, the microstrain values were measured using a strain meter. Comparisons between the two groups were done using t-test, while comparisons between the buccal and palatal areas around the implant were done using paired t-test. Three-way ANOVA was performed to assess factors affecting strain development around implants (P=.05).
RESULTS: The microstrain developed around TRINIA was significantly lower than BioHPP (p <.001).The oblique load leads to higher strain development compared to the axial load. Regarding the oblique load, the strain values were higher in buccal area than the palatal one. CONCLUSION: Strain development around dental implants is influenced by the superstructure material. The oblique occlusal load caused higher microstrain than the axial occlusal load.
KEYWORDS: Dental implant, BioHPP, TRINIA, Strain gauge, Strain development.
RUNNING TITLE: Strain Around Implants using CAD-CAM Reinforced Polymer Superstructures.

---

1 MSc candidate, Department of Prosthodontics, Faculty of Dentistry, Alexandria University, Champolion St., Azarita, Alexandria, 21527, Egypt.
2 Professor, Department of Prosthodontics, Faculty of Dentistry, Alexandria University, Champolion St., Azarita, Alexandria, 21527, Egypt.
3 Lecturer, Department of Prosthodontics, Faculty of Dentistry, Alexandria University, Champolion St., Azarita, Alexandria, 21527, Egypt.

* *Corresponding Author:*
E-mail: Zainab108912013@hotmail.com

INTRODUCTION

Although dental implants are often regarded as the gold standard for teeth replacement, they reveal different biomechanical behaviors than natural teeth as the bone is in intimate contact with the implant due to the absence of periodontal ligaments [1]. This usually leads to bone resorption around dental implants due to the excessive occlusal loads directly transmitted to the surrounding bone [2,3]. Therefore, controlling the transmission of mechanical stresses is crucial for dental implant durability and long-term success [4,5].
One of the significant factors affecting the transmission of stresses between dental implant and bone is the type of restorative material [6,7]. Restorative materials with proper mechanical and physical properties can enhance the long-term success and function of the implant system [8,9]. For decades, metal ceramics as porcelain fused to metal were considered the primary restorative materials for implant-supported crowns. Metals are rigid with modulus of elasticity higher than bone that increased occlusal forces on the implant system without cushioning [10]. However, their disadvantages include marginal gingival discoloration as well as metal allergy [11,12]. Therefore, metal-free dental restorations, such as ceramics, are highly recommended to simulate the natural dentition esthetics [13].
Wherefore zirconia emerged to be used as a substructure for ceramic restorations with high mechanical strength but required veneering to obtain proper esthetics because of their high opacity [14]. These ceramic-ceramic restorations exhibited superior esthetic properties compared with their metal-ceramic counterparts. The success rate of porcelain veneered zirconia restorations has

been reported to be poorer than that of metal-ceramic restorations due to the low fracture strength. Lithium disilicate had higher concentration of crystallin phase and the tighter interlocking matrix of this synthetic glass ceramic that improved the strength and fracture toughness compared with the feldspathic porcelain [15].

However both bilayered, metal ceramic and ceramic fused to zirconia restorations has the technical complication of chipping the veneering ceramic for many reasons including the lower flexural strength of the veneering ceramic [16,17]. Consequently, monolithic restorations were alternative promising restorations which are entirely made of zirconia. Despite their superior esthetic properties, excellent toughness strength and fatigue resistance, ceramics have a high modulus of elasticity that predisposes to high transmission of functional loads to the implant system [18]. In general ceramics are stiff and transmit heavy loads to the implant-prosthesis system resulting in several complications [1,19].

Recently, to mimic the mechanical behavior of the natural tooth, polymer infiltrated ceramic network (PICN) was developed with elastic modulus and hardness that closely matches natural tooth structure than conventional dental composites. It offers comparable fracture toughness to glass ceramics and superior damage tolerance. However, the hardness is reduced and the flexural strength of PICN (130 MPa) is lower than that lithium disilicate glass ceramic material (342 MPa) [20].

Therefore, materials with a low modulus of elasticity, such as Biocompatible High-Performance Polymer (BioHPP), have been introduced [21], The elastic modulus of BioHPP is 4GPa, which closely resembles the elasticity of human bone; and thus, the chewing forces can be cushioned. However, it has a lower load-bearing capacity when compared to zirconia [21]. Its tensile strength and flexure strength is 80MPa and >150MPa respectively [22].

Recently, TRINIA was introduced as a glass fiber reinforced CAD-CAM disc composed of 45wt% epoxy resin matrix and 55wt% multidirectional interlaced glass fibers [22]. Its advantages include biocompatibility, low specific weight, high flexural strength of 393Mpa, and high compressive strength of 374Mpa while BioHPP flexure strength was >150MPa . The modulus of elasticity of TRINIA is 18.8Gpa which is comparable to that of dentin (18.6Gpa) [23]. Using a material with a flexural modulus comparable to dentin and close to human bone allows bending at a similar rate and helps to preserve healthy bone support around the implants; more significantly, this allows the patient to function similarly to when they were dentate.

TRINIA is used as a superstructure material in non-metallic prosthetic restorations, frameworks for anterior or posterior crowns, bridgework, telescopic restorations, framework for fixed restorations and removable partial dentures, three-unit bridges, customized abutments for implants, and implant-supported superstructures [24].

In dental implants, the level of exerted strain affects the biological response of bone [25]. For biomechanical assessment, strain gauge analysis is appropriate as it analyzes the strain quantitatively [26,27]. It is based on assessing the amount of elastic deformation with the least amount of interference possible during testing by applying electrical resistance both in-vivo and in-vitro under static or dynamic loads [28].

Evidence-based clinical and laboratory studies using TRINIA are limited. The aim of the current study was to compare the strain developed around dental implants after using BioHPP and TRINIA as superstructure materials. The null hypothesis was that strain developed around dental implants would not differ among different reinforced polymeric-based implant superstructure materials.

MATERIALS AND METHODS

2.1. Estimation of sample size

Sample size was calculated assuming 80% study power and 5% alpha error. Based on the results of a pilot study conducted on six blocks (3 BioHPP and 3 TRINIA), the mean (SD) strain of BioHPP under axial load was= 261.29 (22.41), and 209.50 (36.12) in case of TRINIA. Based on comparison of means, sample size was calculated to be 7 per group, increased to 8 to make up for laboratory processing errors. The total sample size required= number of groups × number per group= 2 × 8= 16 blocks. Sample size was calculated using G*Power (Version 3.1.9.4)

2.2. Preparation of the study specimen

Sixteen synthetic solid rigid polyurethane test blocks (2x5x4.5 cm) (Aptic Medical, Washington, USA) were used for this study. The blocks were selected as a substitute for human cancellous bone as a test medium for implants installation. Although the material does not have the same structure as the human bone, its mechanical characteristics are similar to human cancellous bone, as defined by the ASTM F-1839-08 standard [29]. It was used in a density of 20 pounds per cubic foot which acts as a substitute for bone types II, III, and IV [30,31].

To fabricate a model of a single tooth replacement (a missing maxillary right first premolar), the crown portion of two ready-made acrylic teeth (representing right maxillary canine and right maxillary second premolar) were sectioned and connected with an 8mm palatal bar made of clay. This distance was to include the implant’s diameter (4mm) as well as 1.5mm on both sides of the implant [32]. A desktop scanner (InEos X5, Dentsply Sirona, Germany) was used to capture the design and construct accurate 3D virtual models of

the dentition on the designing software (Exocad, Germany).
Sixteen final virtual designs were printed out using a 3D printer (Dent 2 Mogassam, Co. LLC, Newark, DE, USA) in dental cast resin (Matte gray ABS-like resin; Phrozen, Taiwan). Cyanoacrylate adhesive was used to attach each tooth model to the polyurethane test blocks.
Cone beam computed tomography was used to scan the bounded saddle replicas. The implant position was virtually planned to be parallel to the long axis of the adjacent teeth by using the designing software (Blue Sky BIO, USA) (Figure 1). To standardize the procedure of implants placement, a surgical guide was fabricated on the final virtual model of the teeth then printed out using a 3D printer (Envision Tec, DDDP, Germany). The printed surgical guide was then placed on the polyurethane blocks, and implants of 4mm in diameter and 10mm in length (*Dentium* Co., Seoul, Korea) (n=16) were then placed. Implants were inserted in the blocks using a torque wrench at 35 Ncm [33].
Titanium straight abutments (*Dentium* Co., Seoul, Korea) of 4.5×5.5-mm for cemented crowns with a 2.5-mm transmucosal area were screwed using an abutment screwdriver and torque wrench with 30Ncm torque (Figure 2) [34].

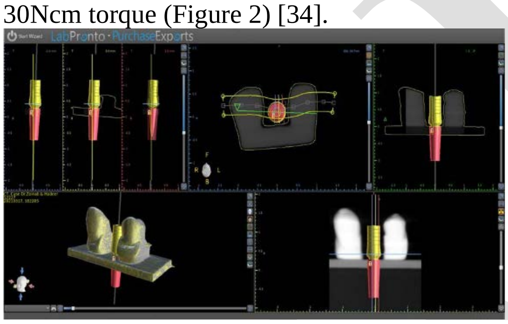

Figure 1: Planning virtual implant design on blue sky software

Figure 2: Titanium abutment insertion

2.3. Fabrication of superstructures

Each abutment was sprayed with scanning spray (CEREC Optispray; Dentsply Sirona, Bensheim, Germany), then scanned with the desktop scanner (InEos X5, Dentsply Sirona, Germany). (Figure 3) illustrates the implant superstructure's final design, which consisted of a BioHPP or TRINIA framework veneered by composite resin. The specimens were divided into two groups according to the framework material: a control group containing BioHPP frameworks (n=8) and a study group with TRINIA frameworks (n=8). CAD software (Exocad, Germany) was used to design the restorative framework with 0.7mm thickness and 80µm cement space. The BioHPP (Bredent, Senden, Germany) and TRINIA (Shofu Dental Corporation, San Marcos, USA) blanks were used to fabricate the specimens of the two groups by using the milling machine (Dentsply Sirona, inLAB MCX5, Germany). Then, the restorative frameworks were checked for their passive fit on the abutments.

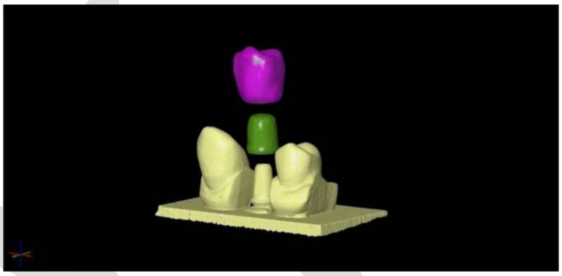

Figure 3: The design of the implant superstructure will be BioHPP or TRINIA framework which is veneered by composite resin crown

Another scan was made for the restorative frameworks with the desktop scanner, and full contour veneering right maxillary first premolar crowns were designed using CAD software program. Composite resin blank (visio.lign; bredent, Germany) was used to fabricate the sixteen veneering crowns. The crowns were checked individually for their passive fit on the restorative framework. The BioHPP and TRINIA restorative framework were prepared for cementation to the veneering crowns using Visio.link adhesive system (Bredent GmbH&Co.KG Senden. Germany).
The Titanium abutments were airborne particles abraded by 110 µm Al_2O_3 particles prior to cementation, then a coat of primer (MKZ primer, Bredent GmbH & Co. KG, Germany) was applied on the abutment and light-cured.
The adhesive surfaces of the cores were airborne-particle abraded with 50-µm Al_2O_3 particles for 15 seconds at a 10-mm distance by an airborne-particle abrasion unit (Basic Classic; Renfert, USA) with a pressure of 0.25 MPa perpendicular to the bonding surface. (35) They were primed using Visio.link primer, then light-cured as well. Each superstructure (framework and veneering crown) was then cemented to the titanium abutment by using an adhesive (DTK adhesive, Bredent GmbH&Co.KG Senden. Germany).

2.4. Load application and strain measurement

Two channels were drilled on the buccal and palatal surfaces of the polyurethane blocks at the implant site, leaving 2mm block thickness covering the implant. Two strain gauge rosettes (Kyowa Electronic Instruments, Japan) were bonded using cyanoacrylate adhesive on the buccal and palatal reduced surfaces of the polyurethane blocks at the level of implant neck where the maximum stress concentration was found [32]. The strain gauge wires were attached to a data acquisition board (Kyowa sensor interface PCD-300A, Japan) installed on a desktop computer. The microvoltage output was adjusted into microstrain via software (PCD 300A; Kyowa Electronic Instruments Co., Ltd.) to give a direct reading. A calibration experiment to the gauges was performed prior to strain measurements to examine the reproducibility of force readings and the gauges' linearity.

A universal testing machine (Lloyd instruments LR 5K, USA) was used to apply axial and oblique static loads on the first premolar crown. Each block was attached to the lower part of the universal testing machine by using 90 degrees custom-made jig, allowing for perpendicular force application to the occlusal plane to simulate the axial load during function. For oblique load application, a 45-degree oblique direction custom-made jig was used. At a constant rate, a single point of 100N static load was applied to the center of the occlusal surface of the crown (Figure 4).

Each measurement was repeated three times for each specimen; the maximum and minimum principal strains were obtained with at least 5 minutes recovery time.

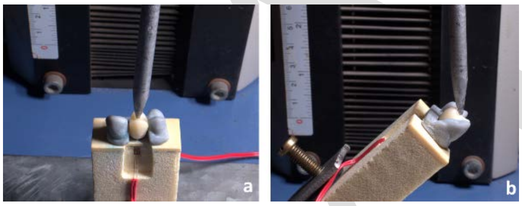

Figure 4: Universal testing machine was used to apply axial static load (100N) at a constant rate, (a) axial force was applied to central fossa of the crown, (b) oblique force was applied to central fossa of the crown.

2.5. Statistical Analysis

Normality was checked for all variables using descriptive statistics, plots (histogram and boxplots), and normality tests. All variables showed normal distribution, so means and standard deviation (SD) were calculated, and parametric tests were used. Comparisons between the two study groups (BioHPP vs. TRINIA) and the two subgroups (axial vs. oblique) were done by using independent samples t-test, while a comparison between the buccal and palatal areas around the implant was done by using paired t-test. Three-way ANOVA was used to assess the effect of superstructure material (BioHPP vs. TRINIA), load (axial vs. oblique), and area (palatal vs. buccal) on the strain development around implants. Adjusted means, 95% confidence intervals (CI), and estimates of effect size (η2) were calculated. Significance was inferred at p value <.05. Data were analyzed using IBM SPSS for Windows (Version 23.0).

RESULTS

Student t-test in table 1 showed that BioHPP group showed significantly greater microstrain values than TRINIA group during different load applications (axial and oblique) at both buccal and palatal areas (p <.001).

Table 1: Comparison of strain developed in the two study groups (BioHPP-TRINIA)
Strain at the palatal and buccal areas in the two study groups at different load directions

		Palatal (n =8)	Buccal (n=8)	Paired t-test P value
		Mean (SD)		
BioHPP	Axial load	402.36 (35.29)	435.54 (38.55)	0.06
	Oblique load	535.49 (27.42)	653.15 (25.57)	<.001*
	T-test P value	<.001*	<.001*	
TRINIA	Axial load	204.65 (22.29)	210.43 (22.08)	0.10
	Oblique load	325.34 (13.49)	453.93 (14.47)	<.001*
	T-test P value	<.001*	<.001*	

Table 2: Comparison of strain developed in the two study groups (BioHPP-TRINIA)
Strain at the palatal and buccal areas in the two study groups after axial and oblique load

		BioHPP (n =8)	**TRINIA (n=8)**	**T-test p value**
		Mean (SD)		
Axial load	**Palatal area**	**402.36 (35.29)**	**204.65 (22.29)**	**<.001***
	Buccal area	**435.54 (38.34)**	**210.43 (22.08)**	**<.001***
Oblique load	**Palatal area**	**535.49 (27.42)**	**325.34 (13.49)**	**<.001***
	Buccal area	**653.15 (27.57)**	**453.93 (14.47)**	**<.001***

Table 2 highlighted that oblique loads resulted in significantly higher microstrain values (p<.001) than axial loads in both groups on both surfaces. Paired t-test showed no significant difference between buccal and palatal microstrain values in both groups when axial load was applied (p= .06 and p= .10) for BioHPP and TRINIA groups, respectively). Conversely, when the oblique load was applied, the microstrain values at the buccal

surface were significantly higher than the palatal surface ($p<.001$) in each study group.
Table 3 highlighted the effect of each parameter on strain development around the implants. It was shown that the three study parameters (superstructure material type, load direction and the area subjected to load) had a significant effect on strain development, however the type of superstructure material showed the highest η^2 (0.90) when compared to load direction and the area of applied load (η^2=0.87 and 0.52, respectively).
Strain at the palatal and buccal areas in the two study groups after axial and oblique load application

DISCUSSION

It has been challenging for the practitioner to decide which restorative material can transmit fewer stresses. The current research attempted to compare the strain developed by TRINIA and BioHPP as implant-supported superstructures. According to the results, the null hypothesis was rejected.
The comparison conducted between Trinia and BioHPP as both are polymer based materials that reduce impact force on implants more than dental ceramics [36]. Different reinforcement types for the two materials make them have different mechanical properties as TRINIA is glass fiber reinforced polymer while BioHPP is ceramic particles reinforced polymer. The modulus of elasticity of TRINIA and BioHPP are comparable to human dentin and bone respectively that may lead to uniform stress distribution and reduce the strain developed on the peripheral bone [23,37,38].
Composite resin veneering was used for improved shock absorption and damping behavior compared with ceramic materials. Therefore they have the ability to dissipate the elastic strain energy [39,40].
The applied load was selected to be ranging from 0 to 100 N as it was below the maximum human masticatory forces [21]. The advanced CAD-CAM technology was used as it has specific criteria for successful dental restorations [41]. Because strain gauges provide quantitative data, they were used to evaluate the strain development in the present study. It was also sensitive, precise, and repeatable during testing [27].
TRINIA group showed significantly lower microstrain values than the control BioHPP group. That might be due to the differences in internal structure between the two materials. TRINIA is a glass fiber reinforced polymer, while BioHPP is a ceramic-reinforced polymer. The relatively low density of the glass fibers in TRINIA enables the material to maintain reinforcement strength properties over a wide range of conditions [30, 31]. Moreover, nano-particle fibers improve the material's mechanical properties, including compressive strength, which is 347 MPa [44].
The elastic modulus of the glass fibers is much higher than that of the matrix polymer. Therefore, forces are mainly directed to the glass fibers, and this has a major role in spread of most of the strain developed before reaching the outer surface (45).

Furthermore, the filler shape plays an important role in stress control as BioHPP has spherical ceramic particles. The spherical-shaped particles might increase stress concentration more than the multidirectional glass fibers of the TRINIA. These glass fibers have a high surface area and are presented in a wavy appearance that helps in decreasing stress through its propagation along the fibers [46]. In addition, the small inter-particle space may help in producing less strain localization [47]. This results in minimal stress transmission to the implant and the surrounding bone.
In addition to that and corroborating the results of this study, Jovanovic et al. [23] reported that glass-fiber reinforced resin-based materials reduced the impact of functional load on the implants up to 50% compared to ceramic reinforced resin-based materials. Also Omaish et al [48] reported that the strain developed around dental implants with 15 and 25 degree angled abutments was significantly lower with TRINIA than BioHPP.
During function, dental implants are subjected to loads with different magnitudes and directions. Considering the load direction, Eric et al. [35] and Chang et al. [36] reported that oblique loads caused higher stress concentration than axial loads in the implant surrounding bone. This is harmonious with the current results showing that the microstrain values recorded during oblique load application were significantly higher than those recorded during axial load application for both groups (TRINIA and BioHPP) at both buccal and palatal areas. This is because axial loads can be compressive on implants, while oblique loads can lead to torsional and lever forces resulting in greater strain and fatigue than the axial one (50).
Results of the current study showed that there were no significant differences between buccal and palatal microstrain values in both groups when the axial load was applied. That might be due to the load being applied in the central fossa and then divided into the buccal and palatal cusps, so there was no stress concentration on one side more than the other [38].
Meanwhile, the buccal microstrain values were significantly higher than the palatal ones during oblique load application in both TRINIA and BioHPP groups as the load direction was from the palatal to the buccal area. Hence, forces were more concentrated on the buccal side. These results agreed with Kaleli et al. [21] , who applied oblique loads directed to the palatal cusp, and reported

higher stress concentration on the palatal side. On the contrary, in our study, the oblique load was directed to the buccal cusp, resulting in higher stress concentration on the buccal side. This can explain the significant increase in microstrain values at the buccal surface in both study groups. Moreover, it also clarifies the non-significant difference between buccal and palatal microstrain values in case of axial load application [38].

The main limitation of the current study is that it did not completely simulate the oral cavity condition. Also, additional long term clinical evaluations are necessary to confirm the current results. The polyurethane blocks have particular bone density and cortical thickness that were homogeneous and isotropic that did not correspond to clinical reality.

CONCLUSION

Based on the study findings and considering the limitations, the following conclusions were drawn: TRINIA superstructure material reduced the amount of strain developed around dental implant when compared to BioHPP. The microstrain recorded during oblique load application was higher than that recorded during axial load. The amount of strain developed is higher in the area where the load is directed.

Conflict of Interest

The authors declare that they have no conflict of interest.

Funding

No funding was received for conducting this study.

Acknowledgement

The authors thank EL Shayeb Dental Lab for their CAD-CAM support, and Dr Noruhan Hussein for her assistance in preparing the statistics of this research.

REFERENCES

1. De Kok P, Kleverlaan CJ, De Jager N, Kuijs R, Feilzer AJ. Mechanical performance of implant-supported posterior crowns. J Prosthet Dent. 2015;114(1):59–66.
2. Abou-Obaid, Ala'a Ibrahim; Al-Otaibi, Hanan Nejer; Akeel RF. Effect of Single Off-Axis Implant Placement on Abutment Screw Stability Under Lateral Loading. Int J Oral Maxillofac Implants. 2016;31(3):520–6.
3. da Silva-Neto JP, Pimentel MJ, das Neves FD, Consani RLX, dos Santos MBF. Stress analysis of different configurations of 3 implants to support a fixed prosthesis in an edentulous jaw. Braz Oral Res. 2014;28(1):67–73.
4. Anitua E, Murias-Freijo A, Flores J, Alkhraisat MH. Replacement of missing posterior tooth with off-center placed single implant: Long-term follow-up outcomes. J Prosthet Dent. 2015;114(1):27–33.
5. Moraschini V, Poubel LADC, Ferreira VF, Barboza EDSP. Evaluation of survival and success rates of dental implants reported in longitudinal studies with a follow-up period of at least 10 years: A systematic review. Int J Oral Maxillofac Surg. 2015;44(3):377–88.
6. Tretto PHW, dos Santos MBF, Spazzin AO, Pereira GKR, Bacchi A. Assessment of stress/strain in dental implants and abutments of alternative materials compared to conventional titanium alloy—3D non-linear finite element analysis. Comput Methods Biomech Biomed Engin. 2020;23(8):372–83.
7. Magne P, Silva M, Oderich E, Boff LL, Enciso R. Damping behavior of implant-supported restorations. Clin Oral Implants Res. 2013;24(2):143–8.
8. Datte CE, Tribst JPM, Dal Piva AM de O, Nishioka RS, Bottino MA, Evangelhista ADM, et al. Influence of different restorative materials on the stress distribution in dental implants. J Clin Exp Dent. 2018;10(5):e439–44.
9. Yalçın Çiftçi; Canay Ş. The Effect of Veneering Materials on Stress Distribution in Implant-Supported Fixed Prosthetic Restorations. Int J Oral Maxillofac Implants. 2000;15(4):571–82.
10. Reda R, Zanza A, Galli M, De Biase A, Testarelli L, Di Nardo D. Applications and Clinical Behavior of BioHPP in Prosthetic Dentistry: A Short Review. J Compos Sci. 2022;6(3):90.
11. Grech J, Antunes E. Zirconia in dental prosthetics: A literature review. J Mater Res Technol. 2019;8(5):4956–64.
12. Takaba M, Tanaka S, Ishiura Y, Baba K. Implant-supported fixed dental prostheses with CAD/CAM-fabricated porcelain crown and zirconia-based framework. J Prosthodont. 2013;22(5):402–7.
13. Jin H ying, Teng M hua, Wang Z jun, Li X, Liang J yue, Wang W xue, et al. Comparative evaluation of BioHPP and titanium as a framework veneered with composite resin for implant-supported fixed dental prostheses. J Prosthet Dent. 2019;122(4):383–8.
14. Pjetursson BE, Valente NA, Strasding M, Zwahlen M, Liu S, Sailer I. A systematic review of the survival and complication rates of zirconia-ceramic and metal-ceramic single crowns. Clin Oral Implants Res. 2018;29(January):199–214.
15. Spitznagel FA, Boldt J, Gierthmuehlen PC. CAD/CAM Ceramic Restorative Materials for Natural Teeth. J Dent Res. 2018;97(10):1082–91.
16. Tezulas E, Yildiz C, Kucuk C, Kahramanoglu E. Current status of zirconia-based all-ceramic restorations fabricated by the digital veneering technique: a comprehensive review. Int J Comput Dent. 2019;22(3):217–30.

17. Farawati F Al, Nakaparksin P. What is the Optimal Material for Implant Prosthesis? Dent Clin North Am. 2019;63(3):515–30.
18. Bijjargi S, Chowdhary R. Stress dissipation in the bone through various crown materials of dental implant restoration: a 2-D finite element analysis. J Investig Clin Dent. 2013;4(3):172–7.
19. Moshaverinia A. Review of the Modern Dental Ceramic Restorative Materials for Esthetic Dentistry in the Minimally Invasive Age. Dent Clin North Am. 2020;64(4):621–31.
20. Xu Z, Yu P, Arola DD, Min J, Gao S. A comparative study on the wear behavior of a polymer infiltrated ceramic network (PICN) material and tooth enamel. Dent Mater. 2017;33(12):1351–61.
21. Kaleli N, Sarac D, Külünk S, Öztürk Ö. Effect of different restorative crown and customized abutment materials on stress distribution in single implants and peripheral bone: A three-dimensional finite element analysis study. J Prosthet Dent. 2018;119(3):437–45.
22. Biris C, Bechir ES, Bechir A, Mola FC, Badiu AV, Oltean C, et al. Evaluations of two reinforced polymers used as metal-free substructures in fixed dental restorations. Mater Plast. 2018;55(1):33–7.
23. Jovanović M, Živić M, Milosavljević M. A potential application of materials based on a polymer and cad/cam composite resins in prosthetic dentistry. J Prosthodont Res. 2021;65(2):137–47.
24. Sulaiman TA. Materials in digital dentistry—A review. J Esthet Restor Dent. 2020;32(2):171–81.
25. Korabi R, Shemtov-Yona K, Dorogoy A, Rittel D. The Failure Envelope Concept Applied to the Bone-Dental Implant System. Sci Rep. 2017;7(1):1–11.
26. Goiato MC, Matheus HR, de Medeiros RA, dos Santos DM, Bitencourt SB, Pesqueira AA. A photoelastic and strain gauge comparison of two attachments for obturator prostheses. J Prosthet Dent. 2017;117(5):685–9.
27. Cozzolino F, Apicella D, Wang G, Apicella A, Sorrentino R. Implant-to-bone force transmission: a pilot study for in vivo strain gauge measurement technique. J Mech Behav Biomed Mater. 2019 Feb 1;90:173–81.
28. Takeshita S, Kanazawa M, Minakuchi S. Stress analysis of mandibular two-implant overdenture with different attachment systems. Dent Mater J. 2011;30(6):928–34.
29. Standard Specification for Rigid Polyurethane Foam for Use as a Standard Material for Testing Orthopaedic Devices and Instruments. Standard ASTM F1839-08, 2021.
30. Di Stefano DA, Arosio P, Gastaldi G, Gherlone E. The insertion torque-depth curve integral as a measure of implant primary stability: An in vitro study on polyurethane foam blocks. J Prosthet Dent. 2018;120(5):706–14.
31. Hoon QCJ, Pelletier MH, Christou C, Johnson KA, Walsh WR. Biomechanical evaluation of shape-memory alloy staples for internal fixation—an in vitro study. J Exp Orthop. 2016;3(1):1–11.
32. Shinya A, Ballo AM, Lassila LVJ, Shinya A, Närhi TO, Vallittu PK. Stress and strain analysis of the bone-implant interface: A comparison of fiber-reinforced composite and titanium implants utilizing 3-dimensional finite element study. J Oral Implantol. 2011;37:133–40.
33. Orban K, Varga E, Windisch P, Braunitzer G, Molnar B. Accuracy of half-guided implant placement with machine-driven or manual insertion: a prospective, randomized clinical study. Clin Oral Investig. 2021;(0123456789).
34. Vinhas AS, Aroso C, Salazar F, Paula L. Review of the Mechanical Behavior of Di ff erent Implant – Abutment Connections. :1–20.
35. Çulhaoğlu AK, Özkır SE, Şahin V, Yılmaz B, Kılıçarslan MA. Effect of Various Treatment Modalities on Surface Characteristics and Shear Bond Strengths of Polyetheretherketone-Based Core Materials. J Prosthodont. 2020;29(2):136–41.
36. Chand YB, Mahendra J, Jigeesh N, Mahendra L, Shivasubramanian L, Perika SB. Comparison of Stress Distribution and Deformation of Four Prosthetic Materials in Full-mouth Rehabilitation with Implants: A Three-dimensional Finite Element Study. J Contemp Dent Pract. 2020;21(11):1210–7.
37. Velho HC, Dalence ET, Machado PS, Rippe MP, Skupien JA, Wandscher VF. Does acid etching prior to applying universal adhesives affect the bond strength of glass fiber post to root dentin? Int J Adhes Adhes. 2021;105(December 2020).
38. Hebert G, Alves É, Silva-sousa YT, Giedra R, Pinelli P, Sousa-neto MD, et al. Mechanical properties and superficial characterization of a milled CAD-CAM glass fiber post. J Mech Behav Biomed Mater. 2018;82:187–92.
39. Rayyan MM, Abdallah J, Segaan LG, Bonfante EA, Osman E. Static and Fatigue Loading of Veneered Implant-Supported Fixed Dental Prostheses. J Prosthodont. 2020;29(8):679–85.
40. Madeira S, Gasik M, Souza JCM, Silva FS, Henriques B. Damping and mechanical behavior of metal-ceramic composites applied to novel dental restorative systems. J Mech Behav Biomed Mater. 2019;90(September 2018):239–47.
41. Papathanasiou I, Kamposiora P, Papavasiliou G, Ferrari M. The use of PEEK in digital prosthodontics: A narrative review. BMC Oral Health. 2020;20(1):1–11.
42. Zhang M, Matinlinna JP. E-Glass Fiber Reinforced Composites in Dental Applications. Silicon. 2012;4(1):73–8.

43. Vallittu P, Matinlinna J. Types of FRCs used in dentistry [Internet]. Clinical Guide to Principles of Fiber-Reinforced Composites in Dentistry. Elsevier Ltd; 2017. 11–34 p.
44. Yu SH, Cho HW, Oh S, Bae JM. Effects of glass fiber mesh with different fiber content and structures on the compressive properties of complete dentures. J Prosthet Dent. 2015;113(6):636–44.
45. Jones FR, Huff NT. Structure and properties of glass fibres. In: Handbook of Tensile Properties of Textile and Technical Fibres. 2009. p. 529–73.
46. Kundie F, Azhari CH, Muchtar A, Ahmad ZA. Effects of filler size on the mechanical properties of polymer-filled dental composites: A review of recent developments. J Phys Sci. 2018;29(1):141–65.
47. Eric P, Seckinger RJ, Kilgren LM. Evaluating parameters of osseointegrated dental implants using finite element analysis- A two-dimensional comparative study examining the effects of implant diameter, implant shape, and load direction. J Oral Implantol. 1998;24(2):80–8.
48. Omaish HHM, Abdelhamid AM, Neena AF. Comparison of the strain developed around implants with angled abutments with two reinforced polymeric CAD-CAM superstructure materials: An in vitro comparative study. J Prosthet Dent. 2022;1–8.
49. Chang C-L, Chen C-S, Yeung TC, Hsu M-L. Biomechanical effect of a zirconia dental implant-crown system: a three-dimensional finite element analysis. Int J Oral Maxillofac Implants. 2012;27(4):e49-57.
50. Silveira MPM, Campaner LM, Bottino MA, Nishioka RS, Borges ALS, Tribst JPM. Influence of the dental implant number and load direction on stress distribution in a 3-unit implant-supported fixed dental prosthesis. Dent Med Probl. 2021;58(1):69–74.
51. de Faria Almeida DA, Pellizzer EP, Verri FR, Santiago JF, de Carvalho PSP. Influence of Tapered and External Hexagon Connections on Bone Stresses Around Tilted Dental Implants: Three-Dimensional Finite Element Method With Statistical Analysis. J Periodontol. 2014;85(2):261–9.

131